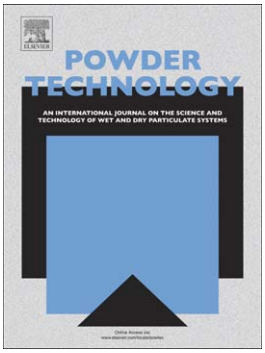

Influence of shape and surface charge on the sedimentation of spheroidal, cubic and rectangular cuboid particles

Neepa Paul, Simon Biggs, Jessica Shiels, Robert B. Hammond, Michael Edmondson, Lisa Maxwell, David Harbottle, Timothy N. Hunter

PII: S0032-5910(17)30723-4
DOI: doi:10.1016/j.powtec.2017.09.002
Reference: PTEC 12806

To appear in: *Powder Technology*

Received date: 20 March 2017
Revised date: 5 August 2017
Accepted date: 1 September 2017

Please cite this article as: Neepa Paul, Simon Biggs, Jessica Shiels, Robert B. Hammond, Michael Edmondson, Lisa Maxwell, David Harbottle, Timothy N. Hunter, Influence of shape and surface charge on the sedimentation of spheroidal, cubic and rectangular cuboid particles, *Powder Technology* (2017), doi:10.1016/j.powtec.2017.09.002

Influence of shape and surface charge on the sedimentation of spheroidal, cubic and rectangular cuboid particles

Neepa Paul[a], Simon Biggs[a,b], Jessica Shiels[a], Robert B. Hammond[a], Michael Edmondson[c], Lisa Maxwell[d], David Harbottle[a], Timothy N. Hunter[a,*]

[a] School of Chemical and Process Engineering, University of Leeds, Leeds, LS2 9JT, UK
[b] School of Chemical Engineering, University of Queensland, Brisbane, 4072, Australia
[c] National Nuclear Laboratory, Central Laboratory, Sellafield, CA20 1PG, UK
[d] Sellafield Ltd, Sellafield, CA20 1PG, UK

*Corresponding author, email: t.n.hunter@leeds.ac.uk, phone: +44(0)1133432790

Key words: Sedimentation; hindered settling; agglomeration; non-spherical colloids; zirconium molybdate; extended Stokes

Abstract

This study investigated the complex settling behaviour of colloidal particles with varied surface charge and shape factors, of specific relevance to nuclear waste processing. Caesium phosphomolybdate (CPM), zirconium molybdate (ZM) and zirconium citromolybdate (ZMCA) were firstly synthesised, producing spheroidal, cubic and rectangular cuboidal morphologies respectively, and compared to agglomerated titania. While zeta-potential measurements indicated all simulant particles attained low isoelectric points, surface group leaching rendered suspensions very acidic, with CPM around its IEP, and ZM/ZMCA stable and positively charged. In sedimentation tests at various concentrations in water and 2 M HNO_3, CPM and titania were found to settle with extremely high hindered settling exponents, consistent with aggregated structures. Exponents for ZM and ZMCA in water were both also well above values for spherical particles; however, this was assumed to be due to heightened drag effects from relative shape factors, rather than aggregation. ZMCA in particular showed a very high exponent of ~11.4, due to the propensity for the rod-like particles to settle in a flat conformation. For ZM in acid, double layer compression from the high electrolyte aggregated the dispersions, correlating to a significant increase in the settling exponent. An extended Stokes relationship was additionally used to understand theoretical limits of shape and aggregation on particle size prediction from hindered settling curves. Importantly, calculated sizes were consistent for the stable ZM and ZMCA in water, despite their non-sphericity and enhanced drag. The relationship failed however with agglomerated suspensions, highlighting its application as a general stability test for sedimenting dispersions.

1 Introduction

Characterising the settling behaviour of particulate suspensions is a critical step in understanding the stability profiles of multiphase systems (both manufactured and natural), as well as optimising many solid-liquid separation operations [1]. For example, settling rate information is critical to quantifying the efficiency of gravity separators in water and minerals processing [2, 3], while analysing the long term sedimentation profiles of emulsions and dispersions in the pharmaceutical, personal care and foods industries, helps determine lifetime product changes [1, 4-6]. Significant fundamental knowledge of settling dynamics, fluid drag and particle-fluid interactions can be extrapolated from changes in measured settling velocities, for a wide variety of systems from dilute free settling to highly hindered sedimentation [7-9], in both Newtonian and non-Newtonian fluids (e.g. [10-12]).

A key aspect of analysis for industrial systems, is how significantly the settling velocity reduces due to hindered fluid effects as particle concentration is increased. While a number of semi-empirical relationships have been derived; such as the Vesilind exponential [13-16] or parameterised hindered settling models, [9, 17-19] perhaps the most widely used correlations are based on the Richardson and Zaki power-law relationship [20] (although a number of modern augmentations also exist, e.g. [15, 21]). Here, at its simplest, the reduced linear settling velocity of a suspension is related to the porosity (1- ϕ, the particle volume fraction) and a defined power-law number exponent 'n', which has dependency on the number of particle and fluid factors [8, 16].

The role of particle shape on hindered settling exponents has been a focus of previous studies, where evidence would suggest that values increase as the particles become less spherical [22-26] due to the enhanced drag. For particles with large aspect ratio, orientation may also be an important factor, where research has shown that rod-like particles in particular may naturally orientate towards a flat conformation of maximum resistance upon settling [11, 23, 27, 28]. Particle de-stabilisation and aggregation in colloidal and mineral systems also critically affects sedimentation dynamics (e.g. [15, 29-32]). In terms of the Richardson-Zaki exponent parameters, it has been shown in a number of investigations that aggregation can lead to values

orders of magnitude larger than observed for stable systems [15, 33-35] and it is empirically possible to link measured values to the size and structure of aggregates [15, 30, 36].

There are a number of approaches to modelling these complex settling systems [1, 2, 7, 37]. Commonly, analytical and numerical methodologies extend Kynch theory [38], through inversion of settling rate-concentration constitutive relationships, which can predict depthwise suspension changes, assuming a series of defined iso-concentration rarefaction lines [2, 7, 39-41]. However, these methods can be mathematically complex, and are difficult to interpret in size/shape polydisperse systems or in suspensions of varying aggregation state. Relatively simpler extended Stokes relationships also exist, which parameterises hindered settling effects on particle fall velocities as a function of particle concentration [30, 36, 42, 43]. While such relationships may be less fundamentally rigorous, ultimately they can derive important information on particle size and structure from the linear settling velocity at various particle volume fractions.

It is clear that the influence of particle shape and aggregation are key determinants in dispersion settling dynamics, and understanding their combined role is critically important for many systems and yet relatively poorly understood. This paper seeks to de-convolute these effects through investigations on particles both academically interesting and industrially important. In particular, we utilize spheroidal, cubic and rectangular cuboidal colloids of caesium phosphomolybdate and zirconium molybdate, which have been previously synthesised [44], as non-active simulants of precipitates produced during the treatment of raffinate from nuclear fuel reprocessing [45-47]. While similar in their bulk chemistry, the distinct shape effects on their sedimentation behaviour were studied in batch settling trials at various concentrations, with results compared to Richardson-Zaki hindered settling fits and an extended Stokes terminal velocity model [42]. Experiments were conducted in both water and 2 M nitric acid (the latter of which mirrors conditions in nuclear operations [48]). Additionally, it is thought that the concentrated acid conditions may dramatically alter the stability of the particles, through changes to pH and the high effective electrolyte concentration.

2 Materials & Methods

2.1 Materials

This study focused on characterising the behaviour of crystalline caesium phosphomolybdate (herein labelled 'CPM' for concision) and zirconium molybdate (herein labelled 'ZM'), which are known to be two of the most significant solids formed during processing of highly active raffinate, which precipitate when acid waste solutions containing certain levels of molybdenum are concentrated, following the removal of uranium and plutonium species [44-47]. Non-active, but chemically similar, CPM and ZM waste simulants, were manufactured according to a procedure outlined previously [44]. Briefly summarised, CPM was synthesised from an inorganic precipitation reaction of phosphomolybdic acid (80% solution, ACROS Chemicals) and caesium nitrate (99.8% purity, Alfer Aesar) dissolved in 2 M nitric acid (Fisher Scientific) maintained at 50 ^{o}C over 48 hr. Post reaction, solids were washed in acid to remove any unreacted reagents and dried.

ZM is formed from a substitution conversion reaction from pre-made CPM. Here, synthesised CPM suspensions were mixed with zirconyl nitrate (Johnson-Matthey) dissolved in 6 M nitric acid at 90 ^{o}C over 2 weeks. Additionally, a modified ZM complex was also synthesised, zirconium citratomolybdate (herein labelled 'ZMCA'), which was formed through addition of citric acid (Fisher Scientific) in the conversion reaction. It is assumed that the citric acid binds to specific surface sites, creating a citratomolybdate complex that alters the crystalline growth rates of certain planes, augmenting crystal morphology. It has been proven previously, that this process creates crystals that are chemically identical to ZM [44]. Both ZM and ZMCA were washed with 2 M nitric acid post-reaction to remove any non-reacted zirconium salt and were additionally washed with ammonium carbamate, to dissolve any non-reacted CPM and dried.

Fumed 99.8% pure anatase type titanium dioxide, 'titania' (Degussa) was also studied, as a commercially available analogue to the synthesised simulant particles.

2.2 Methods

2.2.1 Particle characterisation

Dry particle shape and size was characterised using a LEO/Zeiss 1530 scanning electron microscopy (SEM) (LEO Elektronmikroskope GmbH, Germany). Each sample was dried and

then coated with platinum before being imaged. Select images were digitised with *Image J* software to quantify size and shape characteristics.

A Mastersizer 2000 (Malvern Instruments Ltd., UK) was also used to obtain particle size distribution information for liquid dispersions of the TiO_2 and nuclear simulants. For each sample tested, particulate solids (at ~2 wt%) were well mixed in pH-neutral water for 30 min, and a few drops of the stock dispersions were added to a water-filled, stirred measuring cell mixed at 2000 rpm. Each sample was analysed over 10 s and 10 repeat measurements were carried; the average of these 10 measurements are presented in the paper.

Particle zeta-potentials for all species were measured with a Nanosizer ZS (Malvern Instruments Ltd., UK). Dispersions at a concentration of 1000 ppm, were made for all species, and well mixed under sonication for 30 min. 10^{-4} M potassium nitrate (KNO_3) was used as a background electrolyte in all cases. Zeta-potential averages from 10 measurements were taken at various dispersion pH, altered either using potassium hydroxide (KOH) or nitric acid (HNO_3).

Particle density was measured using an AccuPyc 1330 helium pycnometer (Micromeritics Instrument Corporation, US). The input weight of the solids were measured, and density is determined by the pressure change of helium in a calibrated volume.

2.2.2 Settling studies

The sedimentation rate as a function of volume fraction for all species, was determined using a Turbiscan® (Formulaction, Ramonville, France), as reported elsewhere [15, 48]. Here, 20 mL of well mixed particle dispersions, were placed in a cylindrical glass measurement cell. Backscattered light intensity measurements (at 45^o) were taken through its entire length, as a function of time, to establish sedimentation profile of the particles under gravity. In a typical experiment, samples were left to run for 3 hr 30 min, and data was collected every 2 min. The suspension sediment interface at each time interval was determined from a defined reduction in the threshold backscatter intensity. Particle fractions of 2 – 20 vol% were investigated.

3 Results & Discussion

3.1 Particle characterisation

Scanning Electron Microscopy (SEM) images highlighting the shape of the titania, CPM, ZM and ZMCA are shown in Fig. 1 (a-d). The CPM appear as 'spheroidal' particles (although not completely spherical) of a few hundred nanometres to micron in size. Previous investigation on their growth mechanism [44], indicated that they form from initial small nanometre crystallites that fuse together creating a slightly 'raspberry type' morphology. The ZM and ZMCA are individual crystals of approximately a few microns, with the ZM displaying clear cubic formation, while the ZMCA is an elongated rectangular cuboidal shape. The titania by contrast appears as highly agglomerated clusters of nanocrystals, and while the nature of the aggregates are difficult to interpret under SEM because of capillary drying effects, such complex structuring is commonly found in similar systems [6, 48, 49], from the high temperature sintering that occurs in production.

The Mastersizer particle size distributions (PSDs) for all four particles are shown in Fig. 2. While sizes appear to compare relatively well with SEMs given in Fig. 1, it is emphasised that the distributions for ZM and ZMCA are only qualitative, due to the theoretical interpretation of spherical scattering by the instrument. Hence, to gain some more quantitative information on the ZM and ZMCA particles, size analysis was completed on a number of digitally processed SEM images using *Image J* software, using a minimum of 100 particle measurements. For ZM particles, the cubic length of the particles was measured and size interpreted as the volume equivalent sphere diameter (the diameter of a sphere with the same volume as each cube). As the thickness of the ZMCA were not clearly resolved in the SEM images (from a lack of z-plane resolution), volume equivalence could not be calculated for these particles. Hence, the maximum length was simply measured as a representative diameter. Non-normalised number PSDs for ZM and ZMCA from SEM analysis are shown in Fig. 3, with both volume equivalent and maximum length diameters shown for ZM in (a) and the maximum length diameter shown for ZMCA in (b).

Both the ZM volume equivalent and maximum length diameters presented in Fig. 3 (a) appear internally consistent to the Mastersizer results shown in Fig. 2 (although the sub-micron finer particles were difficult to resolve with the SEM analysis). These results broadly highlight the geometric similarity between equivalent diameters of spheres and cubes, as in effect, the

Mastersizer also measures the sphere equivalent volume diameter. The maximum length diameters measured from ZMCA (Fig. 3 (b)) are larger than the Mastersizer averages, as would be expected [50], with peak averages of 4 – 5 μm. The aspect ratio was also measured for ZMCA from the SEM images to be ~6.

The zeta potential was measured for CPM, ZM and ZMCA systems with results given in Fig. 4. All species exhibit very low pH isoelectric points (IEPs), with the IEP for CPM in particular being only around pH ~1.5 (just outside of the maximum measureable range) while the IEPs for ZM and ZMCA are around pH 3 and 4, respectively. The slight differences between ZM and ZMCA are interesting, owing to the fact that they are chemically identical in the bulk [44, 47]. The only modification comes from the surface adsorption of citric acid, which leads a complex formation on particular surfaces, retarding the growth of those planes, resulting in the rod like confirmation [44]. A secondary effect of the citric acid is that it appears to alter the surface chemistry of the crystals, perhaps lowering affinity for hydroxide bonding leading to a slightly higher IEP.

While there is no previous literature on the zeta potentials of these species, similar large negative potentials across a broad pH range have been reported for $SrMoO_4$ particles [51]. Also, there are correlations to very low IEPs measured with molybdenite (MoS_2) a similar compound to the molybdate species, with sulphur in place of oxygen [52, 53]. In the case of molybdenite, surface groups can react with the water forming negative MnO_4^{2-} ions that dominate the interaction potential. Alternatively, we believe the surface molybdate groups in the CPM, ZM and ZMCA complexes may partially dissociate to form hydrates in water, perhaps through their bound water groups (as ZM hydrates have been shown previously in literature [54]) which would lead to strong negative charges from OH^- groups, and thus the observed highly negative potentials. If bound water groups were forming hydrate groups on particles, it would be expected that the dispersion would acidify from released H^+ ions. Therefore, to test particles reactivity, the final pH of CPM, ZM and ZMCA dispersions made with particle concentrations from 2 – 8 vol% were tested 48 hr after preparation, and displayed in Fig. 5.

Results suggest high levels of acidification are indeed occurring in all species, especially with CPM and ZM, both of which fall below a pH of 1.5 as particle concentration goes beyond 4 vol%. Interestingly, the acid leaching infers some contrasting stability for these systems in

concentrations relevant to the settling studies. Despite the very low IEP of CPM, Fig. 5 indicates that the dispersion pH may in fact be very close to this value for most particle concentrations, and thus some aggregation will likely occur. In contrast, acid leaching may lead to the ZM and ZMCA attaining stable positive charges, as the equilibrium pH is below their associated IEPs. It is also noted that no mass loss was observed in any of these systems over the same time scale, highlighting that while the pH changes, no measureable dissolution of the bulk particles is occurring. This result may further suggest that the pH changes are likely from hydration reactions with bound surface groups.

The zeta potential of titania at various pH is shown in the Supplementary Materials, Fig. S1 in comparison to ZM. Unlike with the highly active simulant particles, the pH for settling TiO_2 systems was stable at around (neutral) pH 7. From Fig. S1, this value correlates approximately to the IEP, and is consistent with literature values [30, 55]. Hence, both the titania and CPM may similarly be presumed to be around their respective IEPs, although at very different equilibrium pH.

3.2 Settling Studies

To understand the expected differences in sedimentation between water and acid systems, the Stokes equation [5, 50, 56] was used to theoretically estimate the free settling velocities in dilute systems. The mean particle sizes measured from the Mastersizer (Fig. 2) were used in the calculation for all species. Particle densities were measured with the pycnometer to be 3.82, 3.41 and 3.41 g/mL for CPM, ZM and ZMCA respectively, while the density of the anatase titania was taken to be 3.78 g/mL (as standard). Water density and viscosity were taken as for standard temperature and pressure, while fluid properties for the 2 M nitric acid solutions were taken from literature (giving an acid solution density of 1070 kg/m^3 and viscosity of ~1.2 mPas [57, 58]). Estimated terminal settling velocities are compared for all systems in Fig. 6.

The calculated rates in Fig. 6 indicate that all particles should have slightly lower settling rates in nitric acid (with a reduction of ~ 20%, from the increased density and viscosity of the fluid) and also, using the measured size means, settling rates are expected to be much lower for the titania and CPM, because of their much smaller sizes. It is appreciated however that comparisons are only qualitative, as the Stokes equation itself assumes a spherical particle shape for drag, which is clearly not the case for ZM and ZMCA. Indeed, it is generally known

that drag increases as shape becomes less spherical, especially for particles with high aspect ratio [23, 26, 59] and thus expected drag coefficients for ZM and ZMCA would be higher than for the spheroidal CPM, suggesting the Stokes equation may over estimate their respective settling velocities. For ZMCA in particular, drag may be significantly increased, especially if particles orientate towards a flat conformation of maximum drag resistance upon settling [11, 27, 28].

The sedimentation behaviour was quantitatively compared through the Turbiscan measurements, where the interfacial linear settling rate was measured for all particle systems at concentrations of 2 to 20 vol%, and are shown in Fig. 7 (a) and (b) (in water and 2 M nitric acid respectively). Dotted lines represent exponential Richardson-Zaki power law fits for each species (to be discussed in relation to Figs. 8 and 9 following). The raw interface versus time plots (measured from the Turbiscan backscatter) are shown for all systems in the Supplementary Materials, Fig. S2 (water) and Fig. S3 (acid). It is also noted that because of a lack of synthesised ZMCA material, there was not adequate quantity to run settling tests for this particle type in acid, and only water results are reported.

Data for the lowest particle concentrations of 2 vol% given in Fig. 7 may be related to the theoretical settling rate predictions in Fig. 6, as it is assumed concentration is low enough to, at least, approach a dilute environment. It is immediately obvious upon comparisons of Fig. 7 (a) (water studies) that the settling rates of TiO_2 and ZM in water at 2 vol%, are approximately an order of magnitude higher than estimated with the Stokes equation. This result suggests that extensive aggregation has occurred with TiO_2 and CPM, likely due to both being near their respective IEPs. For the ZM and ZMCA in water, settling rates of the low 2 vol% dispersions are closer to predictions, given the significant limitations of the Stokes estimations from their non-sphericity. For settling in acid (Fig. (b)), it is clear that while sedimentation rates for the 2 vol% TiO_2 and CPM suspensions are slightly reduced, as expected, the rate for the 2 vol% ZM suspension is in fact higher than that in water. This behaviour suggests that aggregation may also be occurring for the ZM systems in acid, with increased settling rates to compensate for the increased fluid density and viscosity.

To understand the role of particle aggregation on settling dynamics more quantitatively, settling data was analysed using the standard (non-modified) Richardson-Zaki (RZ) power-law hindered settling model [8, 20, 60]. Linearized fits are shown for the settling rate data for TiO_2,

CPM, ZM and ZMCA in Fig. 8 (a)-(d) respectively, where the natural log of the measured settling rate (u) is plotted in terms of the natural log of porosity (ε). It is noted that these fits are also represented in Fig. 7 by the dotted lines.

A number of important aspects on the influence of particle shape and aggregation state on suspension settling, can be ascertained from associated exponent values calculated from fit slopes in Fig. 8. The exponents for TiO_2 and CPM (at 51.5 and 39 respectively) are an order of magnitude larger than the standard value of ~4.65, which is often quoted for non-aggregated spherical systems [8, 16, 20]. While these values are considerably above those found with stable dispersions, such large deviation is consistent with exponents reported for coagulated mineral systems [15, 33-35] and again infer a high degree of aggregation in both CPM and TiO_2 dispersions.

Fit values for ZM and ZMCA (with exponents of 9.8 and 13.6 respectively) are still substantially larger than expected for spherical particles. However, previous literature has shown distinct increases in exponent values even for well dispersed systems with non-spherical particles [22, 24] especially with higher aspect ratio [23, 25]; although, the measured values in this case are still above those generally reported. Nevertheless, given the indication of stability from size and zeta potential measurements, along with the qualitative correlation of settling rates to Stokes estimations, it is believed these values do represent those of stable dispersions with enhanced drag. The small size of these particles in relation to previous studies [22], with resulting high surface area to volume ratio and high number density, could further heighten the hindered settling effects in these systems. Indeed, it would be also expected that stable ZMCA particles would have a higher exponent as measured, due to the potential for them to orientate in a flat conformation, heightening the relative drag from their large aspect ratio, as discussed [11, 23, 27, 28].

The settling rate data for TiO_2, CPM and ZM in 2 M acid (shown in Fig. 7 (b)) were also converted to the linearized Richardson-Zaki fits, with results displayed in Fig. 9. The measured exponent for the TiO_2 is similar to the water system (at ~49) inferring similar hindered settling behaviour, while the slope value for CPM at 53 is markedly higher than for water, indicating a higher degree of aggregation leading to enhanced hindered settling effects. For ZM, the increase in the exponent is proportionally even more significant (at ~25, more than double its value in water) which suggests that the ZM has gone from being a stable dispersion to

aggregated as acid is introduced. Importantly, the effect of the 2 M nitric acid will have two competing chemical effects on the suspensions (as well as the main physical change to fluid viscosity, which will also increase drag). Acid will, obviously, push the pH down to low levels (with measured pH values all around -1.2 to -1.3, consistent with the strong acid) where all particles are assumed to attain a positive surface potential, even for the CPM. Conversely, the acid counterions give an extremely high concentration of electrolyte, and thus the electrical double layer will be depressed. Results highlight the action of acid counterions in reducing the EDL, dominating the interaction potential of the particles and leading to high levels of aggregation in all systems.

3.3 Validity assessment of an extended Stokes relationship

There have been a number of previous research studies that have sought to characterise particle size or structural information from hindered settling curves (as recently reviewed by Piazza [1]). For highly aggregated systems, relationships such as suggested by Michaels & Bolger [36] and Valverde *et al.* [43] effectively consider that enhancement to the RZ hindered settling exponents (as qualitatively observed in relation to Figs. 8 and 9) are related to the number density of particles within an aggregate. Such methodologies have recently been reviewed and tested by Johnson and co-workers [15] in coagulated magnesium hydroxide systems.

For non-aggregated systems, there is greater certainty in theoretical approaches that extend the Stokes equation allowing calculation of effective particle settling rates outside of the dilute regime [1, 42, 61, 62]. Such methodologies have the added value of extending gravimetric methods for size determination [4, 5]. As settling data in the current study consist of both well-dispersed and aggregated dispersions, it was decided to assess the validity of an extended Stokes relationship in these complex systems. In particular, the derivation given by Mills and Snabre [42] was used as the basis to calculate the relative changes in estimated particle velocity due to hindered settling effects, and converted to equivalent diameter using the Stokes equation for spheres. The derived formula is given in Eq. 1, where, d_s represents the calculated spherical Stokes diameter, μ the fluid viscosity, (of water or 2 M acid respectively), u_s the measured settling rate in each system, (ρ_p - ρ_l) the difference in particle-fluid density, g the gravitation constant and Φ the particle concentration variable.

$$d_s = \sqrt{\frac{18\mu u_s}{(\rho_p - \rho_l)g} \bullet \frac{1 + 4.6\phi / 1 - \phi^3}{1 - \phi}} \quad (1)$$

Importantly, we note that in Eq. 1, there is an additional constant of *4.6*, which is used to alter the influence of the volume fraction. Mills and Snabre [42] originally gave this as an empirical constant, *k*, but matched it to the value of 4.6 by fitting with other reported experimental data. Interestingly, this value effectively approximates to the generally reported RZ exponent value for hard spheres of 4.65 [8]; although it is not derived identically. Indeed, Valverde and co-workers [43], found fitted values closer to 6.557 in an extension to this equation for cohesive powders, inferring some influence of particle dispersion.

Data was analysed, by taking the measured settling velocities for the systems studied at various concentrations given in Fig. 7, and calculating an estimated extended Stokes diameter for each concentration using Eq. 1. As all measured RZ exponents were much greater than the reported value for hard spheres, it was anticipated that results may lead to some internal dependence error in calculated diameters. However, it is emphasised that the sensitivity of this factor in the equation is relatively low, and because of the differences in derivation between a RZ power-law fit and the given extended Stokes equation, there are questions as to correlation between these values. Nevertheless, this relationship was used to characterise any consistent differences between aggregated and non-aggregated systems, and so to better comprehend the limitation of this extended theory. Bar charts displaying the calculated diameters for TiO_2, CPM and ZM with concentrations from 2 – 20 vol% in water and 2 M nitric acid are shown in Fig, 10 (a-c). Data for the ZMCA for concentrations of 2 – 14 vol% in water only is given in Fig. 10 (d).

The calculated diameters given in Fig. 10 for TiO_2 and CPM appear highly unstable and likely invalid (due to the clear dependency on particle concentration). While estimated sizes are generally larger in the 2 M nitric acid than water (perhaps as expected from a higher degree of aggregation) they are observed to considerably reduce as concentration is increased. This behaviour is likely a mathematical instability, caused by the inability for the given relationship to properly model the increased hindered settling effects from within the aggregation systems, and highlights an important limitation to the application of theoretical expressions for particle velocity estimation in hindered suspensions [15].

Results for ZM and ZMCA alternatively establish a key level of insight in to the use of extended Stokes relationships to correlate dispersion aggregation. Estimated sizes for both ZM and ZMCA in water show high levels of stability (concentration independence) and give consistent sizes that are comparable to those measured (at least considering the aforementioned limitations because of their lack of sphericity). There is a slight drop in estimations for ZMCA at high concentrations, although this perhaps may be down to particle levels approaching the dispersion gel point in this system. Overall however, results show that Eq. 1 can give a robust estimation of particle size from sedimentation data, across a relatively broad concentration envelope. This consistency comes despite the fact that these particles have relatively high hindered settling exponent values for non-aggregated systems.

Additionally, key information can be gained from the ZM data in nitric acid. Estimated size values in this system appear similar to TiO_2 and CPM data (significantly reducing as particle concentration is increased). Such instability would again correlate with the evidence from the zeta-potential curves and dispersion equilibrium pH (Figs. 4 & 5) and the RZ linearized settling data (Figs.8 and 9) that while the ZM particles are a stable dispersion in water, they aggregate due to double layer compression in high acid environments. Hence, Eq. 1 could actually be used as a general test of dispersion aggregation, even in non-spherical systems with high hindered settling exponents, through observations to the concentration independence of calculated sizes.

4 Conclusions

This paper describes work into the characterisation of particulate properties and sedimentation behaviour of non-active nuclear waste simulants, which are precipitated products from nuclear fuel reprocessing, containing variable shape and dispersion properties. Colloidal suspensions of spheroidal CPM, cubic ZM and elongated cuboidal ZMCA, were tested along with commercial fumed anatase titania, in both water and 2 M nitric acid (the latter correlating to waste processing conditions). While all simulant particles had very low measured isoelectric points, surface acid group leaching, which was assumed to occur through partial dissociation of bound water groups, led to very low equilibrium pH in dispersions after 48 hr, significantly altering the associated stability of the simulant particles.

It was found that CPM and TiO_2 systems settled as highly aggregated dispersions, in both water and acid conditions, with very high hindered settling exponents measured. In contrast, ZM and ZMCA systems appeared to settle as stable dispersions in water. While measured hindered settling parameters (at 9.8 and 13.6 respectively) are still above values generally reported for stable systems, the settling data combined with evidence from potential measurements, suggested these values are in fact due to enhancement of drag coefficient from shape effects. For ZM in acid, it appeared that double layer compression from the high electrolyte systems dominated inter-particle forces, aggregating the dispersions, which correlated to a significant increase in the hindered settling parameter.

Additionally, an extended Stokes equation, as proposed by Mills and Snabre [38], was modified to allow the estimation of particle diameters from settling data with particle concentrations of 2 – 20 vol%. Importantly, analysis revealed consistent calculated sizes for ZM and ZMCA in water, across their concentration range, providing strong evidence that the correlation sufficiently estimated hindered settling effects in these systems, despite the non-sphericity of these particles. However, for all aggregated particle systems tested, the model was un-stable (and did not provide concentration independence in calculated diameters) highlighting that the key limitation in the extended Stokes method is not particle shape, but aggregation state. This result also suggested that this method could be used as a specific test for dispersion conditions, and is a useful tool for extracting additional information from gravimetric methods for particle size determination.

Acknowledgements

The authors would like to thank the Engineering and Physical Sciences Research Council (EPSRC) UK, along with Sellafield Ltd. and the National Nuclear Laboratory (NNL) for funding of this project, as part of an Industrial CASE award. NNL is also thanked for industrial management of the project.

References

[1] R. Piazza, Settled and unsettled issues in particle settling, Reports on Progress in Physics, 77 (2014) 056602.

[2] P. Grassia, Y. Zhang, A.D. Martin, S.P. Usher, P.J. Scales, A.H. Crust, R. Spehar, Effects of aggregate densification upon thickening of Kynchian suspensions, Chemical Engineering Science, 111 (2014) 56-72.

[3] T.N. Hunter, S.P. Usher, S. Biggs, P.J. Scales, A.D. Stickland, G.V. Franks, Characterization of bed densification in a laboratory scale thickener,by novel application of an acoustic backscatter system, Procedia Engineering, 102 (2015) 858-866.

[4] C.M. Alexander, J.C. Dabrowiak, J. Goodisman, Gravitational sedimentation of gold nanoparticles, Journal of Colloid and Interface Science, 396 (2013) 53-62.

[5] J.-F. Chen, Y. Luo, J.-H. Xu, Q.-M. Chen, J. Guo, Visualization study on sedimentation of micron iron oxide particles, Journal of Colloid and Interface Science, 301 (2006) 549-553.

[6] Y.-J. Yang, A.V. Kelkar, X. Zhu, G. Bai, H.T. Ng, D.S. Corti, E.I. Franses, Effect of sodium dodecylsulfate monomers and micelles on the stability of aqueous dispersions of titanium dioxide pigment nanoparticles against agglomeration and sedimentation, Journal of Colloid and Interface Science, 450 (2015) 434-445.

[7] P. Garrido, R. Bürger, F. Concha, Settling velocities of particulate systems: 11. Comparison of the phenomenological sedimentation–consolidation model with published experimental results, International Journal of Mineral Processing, 60 (2000) 213-227.

[8] R. Holdich, Fundamentals of Particle Technology, Midland Information Technology and Publishing, Nottingham, 2002.

[9] A.D. Stickland, C. Burgess, D.R. Dixon, P.J. Harbour, P.J. Scales, L.J. Studer, S.P. Usher, Fundamental dewatering properties of wastewater treatment sludges from filtration and sedimentation testing, Chemical Engineering Science, 63 (2008) 5283-5290.

[10] R. Elgaddafi, R. Ahmed, F. Growcock, Settling behavior of particles in fiber-containing Herschel Bulkley fluid, Powder Technology, 301 (2016) 782-793.

[11] J.-P. Hsu, W.-J. Chen, S. Tseng, C.-J. Chen, Sedimentation of a cylindrical particle along the axis of a cylindrical tube filled with Carreau fluid, Powder Technology, 166 (2006) 1-13.

[12] B.A. Moreira, F. de Oliveira Arouca, J.J.R. Damasceno, Analysis of suspension sedimentation in fluids with rheological shear-thinning properties and thixotropic effects, Powder Technology, 308 (2017) 290-297.

[13] A. Vesilind, Design of prototype thickeners from batch settling tests, Water Sewage Works, 115 (1968) 302-307.

[14] C.M. Bye, P.L. Dold, Evaluation of Correlations for Zone Settling Velocity Parameters Based on Sludge Volume Index-Type Measures and Consequences in Settling Tank Design, Water Environment Research, 71 (1999) 1333-1344.

[15] M. Johnson, J. Peakall, M. Fairweather, S. Biggs, D. Harbottle, T.N. Hunter, Analytical characterisation of multiple hindered settling regimes in aggregated mineral suspensions, Industrial & Engineering Chemistry Research, 55 (2016) 9983–9993.

[16] A.E. Stricker, I. Takacs, A. Marquot, Hindered and compression settling: Parameter measurement and modelling, Water Science & Technology, 56 (2007) 101-110.

[17] D.R. Lester, S.P. Usher, P.J. Scales, Estimation of the hindered settling function R(phi) from batch-settling tests, AIChE Journal, 51 (2005) 1158-1168.

[18] S.J. Skinner, L.J. Studer, D.R. Dixon, P. Hillis, C.A. Rees, R.C. Wall, R.G. Cavalida, S.P. Usher, A.D. Stickland, P.J. Scales, Quantification of wastewater sludge dewatering, Water Research, 82 (2015) 2-13.

[19] S.P. Usher, L.J. Studer, R.C. Wall, P.J. Scales, Characterisation of dewaterability from equilibrium and transient centrifugation test data, Chemical Engineering Science, 93 (2013) 277-291.

[20] J. Richardson, W. Zaki, The sedimentation of a suspension of uniform spheres under conditions of viscous flow, Chemical Engineering Science, 3 (1954) 65-73.

[21] P.J.T. Dankers, J.C. Winterwerp, Hindered settling of mud flocs: Theory and validation, Continental Shelf Research, 27 (2007) 1893-1907.

[22] Y.S. Chong, D.A. Ratkowsky, N. Epstein, Effect of particle shape on hindered settling in creeping flow, Powder Technology, 23 (1979) 55-66.

[23] R. Lau, H.K.L. Chuah, Dynamic shape factor for particles of various shapes in the intermediate settling regime, Advanced Powder Technology, 24 (2013) 306-310.

[24] M.R. Tomkins, T.E. Baldock, P. Nielsen, Hindered settling of sand grains, Sedimentology, 52 (2005) 1425-1432.

[25] M.A. Turney, M.K. Cheung, R.L. Powell, M.J. McCarthy, Hindered settling of rod-like particles measured with magnetic resonance imaging, AIChE Journal, 41 (1995) 251-257.

[26] A.S. Dogonchi, M. Hatami, K. Hosseinzadeh, G. Domairry, Non-spherical particles sedimentation in an incompressible Newtonian medium by Padé approximation, Powder Technology, 278 (2015) 248-256.

[27] L. Fan, Z.-S. Mao, C. Yang, Experiment on Settling of Slender Particles with Large Aspect Ratio and Correlation of the Drag Coefficient, Industrial & Engineering Chemistry Research, 43 (2004) 7664-7670.

[28] R. Lau, M.S. Hassan, W. Wong, T. Chen, Revisit of the Wall Effect on the Settling of Cylindrical Particles in the Inertial Regime, Industrial & Engineering Chemistry Research, 49 (2010) 8870-8876.

[29] J. Gustafsson, E. Nordenswan, J.B. Rosenholm, Consolidation behavior in sedimentation of TiO_2 suspensions in the presence of electrolytes, Journal of Colloid and Interface Science, 258 (2003) 235-243.

[30] E. Iritani, T. Hashimoto, N. Katagiri, Gravity consolidation–sedimentation behaviors of concentrated TiO_2 suspension, Chemical Engineering Science, 64 (2009) 4414-4423.

[31] J.S. Vesaratchanon, A. Nikolov, D.T. Wasan, Sedimentation of concentrated monodisperse colloidal suspensions: Role of collective particle interaction forces, Journal of Colloid and Interface Science, 322 (2008) 180-189.

[32] Y.-J. Yang, A.V. Kelkar, D.S. Corti, E.I. Franses, Effect of Interparticle Interactions on Agglomeration and Sedimentation Rates of Colloidal Silica Microspheres, Langmuir, 32 (2016) 5111-5123.

[33] K.S. Alexander, D. Dollimore, S.S. Tata, V. Uppala, A Comparison of the Coefficients in the Richardson and Zaki's and Steinour's Equations Relating to the Behavior of Concentrated Suspensions, Separation Science and Technology, 26 (1991) 819-829.

[34] M. Bargieł, E.M. Tory, Extension of the Richardson–Zaki equation to suspensions of multisized irregular particles, International Journal of Mineral Processing, 120 (2013) 22-25.

[35] R.M. Turian, T.W. Ma, F.L.G. Hsu, D.J. Sung, Characterization, settling, and rheology of concentrated fine particulate mineral slurries, Powder Technology, 93 (1997) 219-233.

[36] A.S. Michaels, J.C. Bolger, Settling Rates and Sediment Volumes of Flocculated Kaolin Suspensions, Industrial & Engineering Chemistry Fundamentals, 1 (1962) 24-33.

[37] R. Silva, F.A.P. Garcia, P.M.G.M. Faia, M.G. Rasteiro, Settling Suspensions Flow Modelling: A Review, KONA Powder and Particle Journal, 32 (2015) 41-56.

[38] G.J. Kynch, A theory of sedimentation, Transactions of the Faraday Society, 48 (1952) 166-176.

[39] R. Bürger, F. Concha, K.K. Fjelde, K.H. Karlsen, Numerical simulation of the settling of polydisperse suspensions of spheres, Powder Technology, 113 (2000) 30-54.

[40] R. Dorrell, A.J. Hogg, Sedimentation of bidisperse suspensions, International Journal of Multiphase Flow, 36 (2010) 481-490.

[41] B.B.G. van Deventer, S.P. Usher, A. Kumar, M. Rudman, P.J. Scales, Aggregate densification and batch settling, Chemical Engineering Journal, 171 (2011) 141-151.

[42] P. Mills, P. Snabre, Settling of a suspension of hard spheres, Europhysics Letters, 25 (1994) 651.

[43] J.M. Valverde, M.A.S. Quintanilla, A. Castellanos, P. Mills, The settling of fine cohesive powders, Europhysics Letters, 54 (2001) 329.

[44] N. Paul, R.B. Hammond, T.N. Hunter, M. Edmondson, L. Maxwell, S. Biggs, Synthesis of nuclear waste simulants by reaction precipitation: Formation of caesium phosphomolybdate, zirconium molybdate and morphology modification with citratomolybdate complex, Polyhedron, 89 (2015) 129-141.

[45] D.N. Bykhovskii, T.I. Kol'tsova, M.A. Kuz'mina, Phases of variable composition in crystallization of cesium phosphomolybdate, Radiochemistry, 48 (2006) 429-433.

[46] J. Jiang, I. May, M.J. Sarsfield, M. Ogden, D.O. Fox, C.J. Jones, P. Mayhew, A Spectroscopic Study of the Dissolution of Cesium Phosphomolybdate and Zirconium Molybdate by Ammonium Carbamate, Journal of Solution Chemistry, 34 (2005) 443-468.

[47] B. Dunnett, T. Ward, R. Roberts, J. Cheesewright, Physical Properties of Highly Active Liquor Containing Molybdate Solids, Procedia Chemistry, 21 (2016) 24-31.

[48] N. Paul, S. Biggs, M. Edmondson, T.N. Hunter, R.B. Hammond, Characterising highly active nuclear waste simulants, Chemical Engineering Research and Design, 91 (2013) 742-751.

[49] J. Bux, J. Peakall, S. Biggs, T.N. Hunter, In situ characterisation of a concentrated colloidal titanium dioxide settling suspension and associated bed development: Application of an acoustic backscatter system, Powder Technology, 284 (2015) 530-540.

[50] M. Konert, J.E.F. Vandenberghe, Comparison of laser grain size analysis with pipette and sieve analysis: a solution for the underestimation of the clay fraction, Sedimentology, 44 (1997) 523-535.

[51] J. Mukherjee, D.P. Dutta, J. Ramakumar, A.K. Tyagi, A comprehensive study on the uptake of dyes, Cu(II) and radioactive 137Cs(I) by sonochemically synthesized strontium/yttrium tungstate and molybdate nanoparticles, Journal of Environmental Chemical Engineering, 4 (2016) 3050-3064.

[52] Z. Lu, Q. Liu, Z. Xu, H. Zeng, Probing Anisotropic Surface Properties of Molybdenite by Direct Force Measurements, Langmuir, 31 (2015) 11409-11418.

[53] J.O. Tabares, I. Madrid Ortega, J.L. Reyes Bahena, A.A. Sanchez Lopez, D. Valdez Perez, A. Lopez Valdivieso, Surface properties and floatability of molybdenite, China-Mexico Workshop on Minerals Particle TechnologySan Luis Potosi, Mexico, 2006.

[54] A. Magnaldo, M. Masson, R. Champion, Nucleation and crystal growth of zirconium molybdate hydrate in nitric acid, Chemical Engineering Science, 62 (2007) 766-774.

[55] M. Kosmulski, S. Durand-Vidal, J. Gustafsson, J.B. Rosenholm, Charge interactions in semi-concentrated titania suspensions at very high ionic strengths, Colloids and Surfaces A: Physicochemical and Engineering Aspects, 157 (1999) 245-259.

[56] G.G. Stokes, On the effect of the internal friction of fluids on the motion of pendulums, Transactions of the Philosophical Cambridge Society 9(1851) 51-52.

[57] F.H. Rhodes, H.B. Hodge, Viscosity Relationships in the System Sulfuric Acid-Nitric Acid-Water, Industrial & Engineering Chemistry, 21 (1929) 142-150.

[58] S. Thomas, Density of nitric acid, Wissen Scientific - https://wissen.science-and-fun.de/chemistry/chemistry/density-tables/density-of-nitric-acid/, Accessed 6-2016.

[59] A. Haider, O. Levenspiel, Drag coefficient and terminal velocity of spherical and nonspherical particles, Powder Technology, 58 (1989) 63-70.

[60] A. Maude, R. Whitmore, A generalized theory of sedimentation, British Journal of Applied Physics, 9 (1958) 477.

[61] G.K. Batchelor, C.S. Wen, Sedimentation in a dilute polydisperse system of interacting spheres. Part 2. Numerical results, Journal of Fluid Mechanics, 124 (1982) 495-528.

[62] R.H. Davis, H. Gecol, Hindered settling function with no empirical parameters for polydisperse suspensions, AIChE Journal, 40 (1994) 570-575.

<u>Collated Figures Document</u> – N. Paul *et al.* "Influence of shape and surface charge on the sedimentation of spheroidal, cubic and rectangular cuboidal particles"

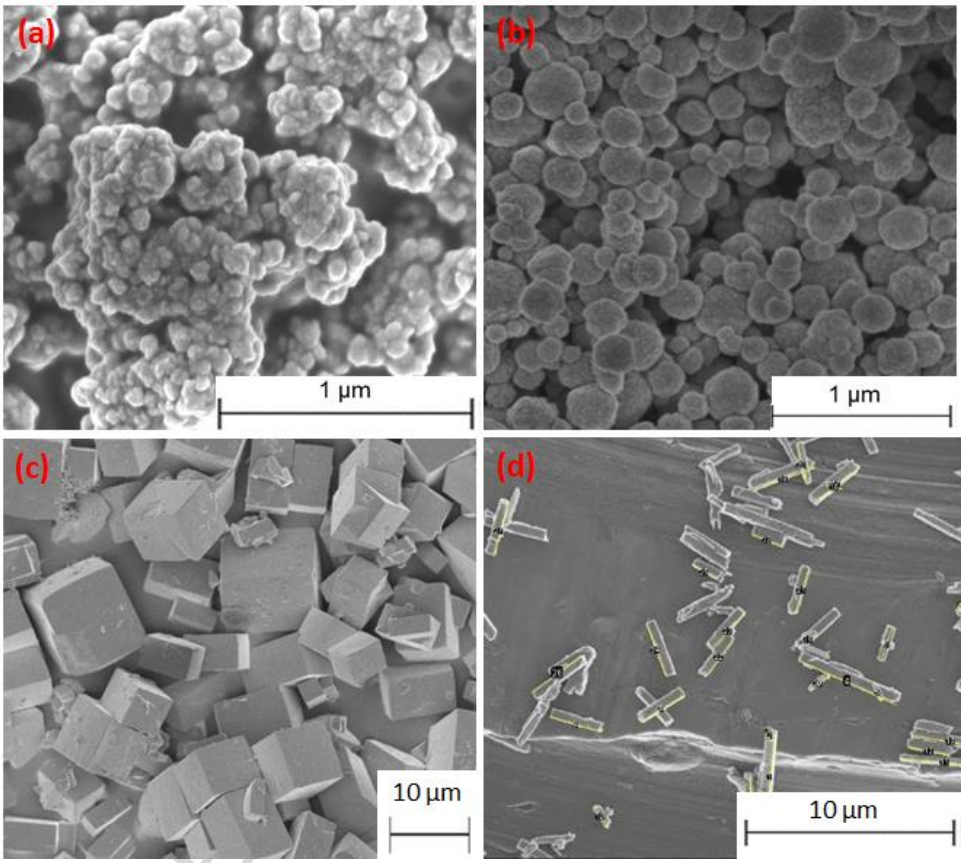

Figure 1: Scanning electron micrographs (SEMs) of simulant particles at various magnifications; (A) TiO_2 at 45k, (B) CPM at 29.32k, (C) ZM at 1.74k and (D) ZMCA at 6.74k. Annotated lines in 'D' represent length segments visualised with *Image J*.

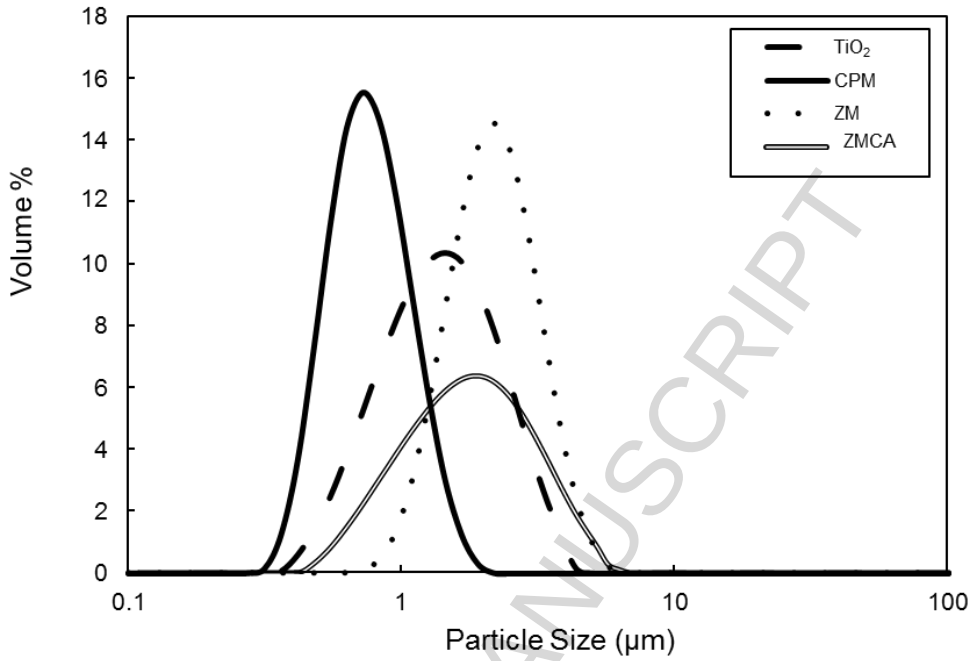

Figure 2: Particle size distributions (volume weighted) for all simulant particles.

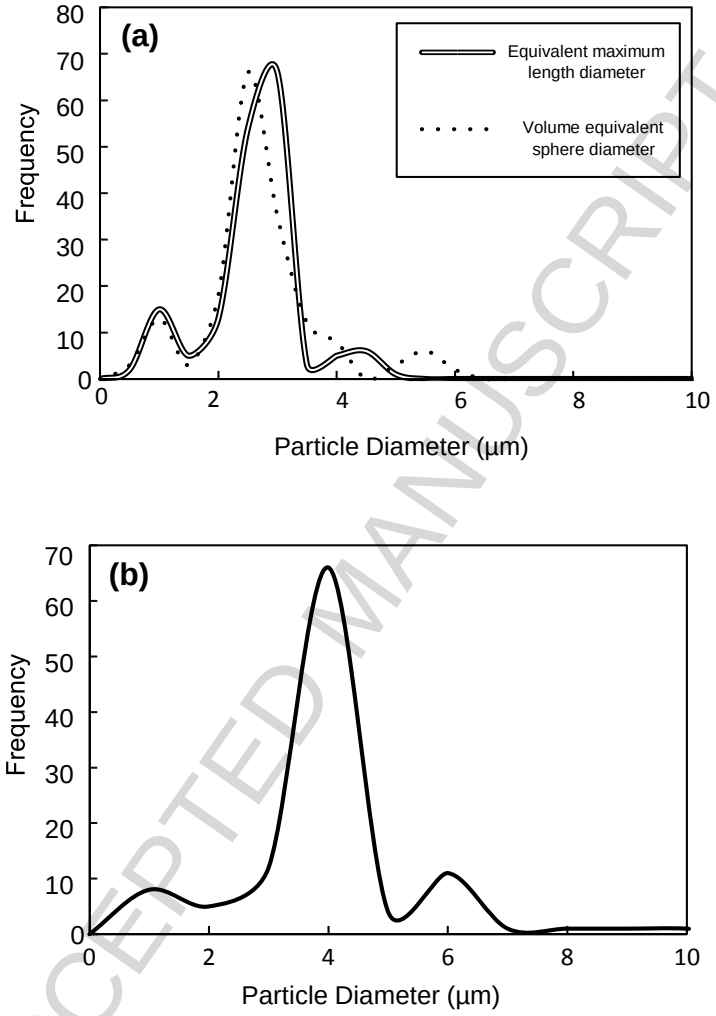

Figure 3: Particle size distributions from image analysis of SEMs (using a minimum of 100 particles) showing (a) volume equivalent and maximum length equivalent diameters of synthesised ZM and (b) maximum length equivalent diameter of ZMCA particles.

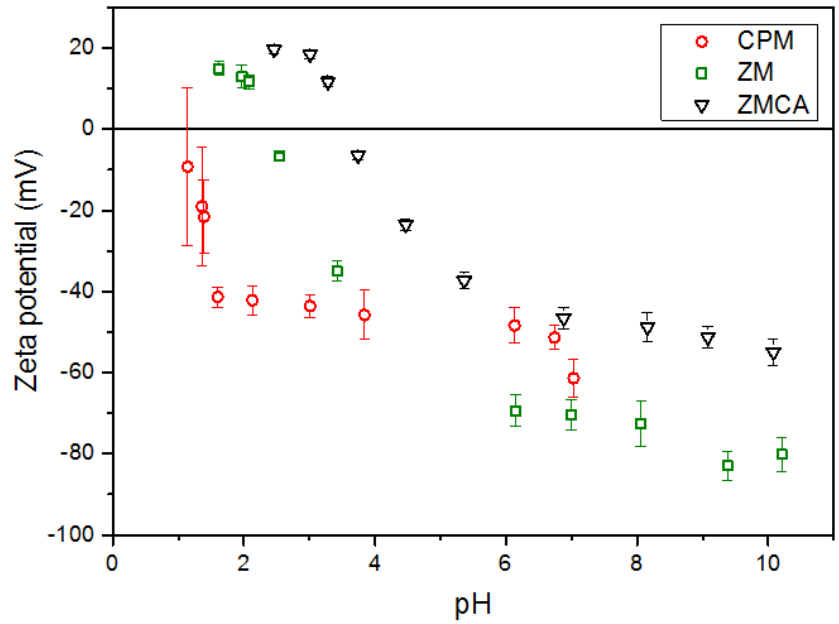

Figure 4: Zeta-potentials of CPM, ZM and ZMCA particles at various pH.

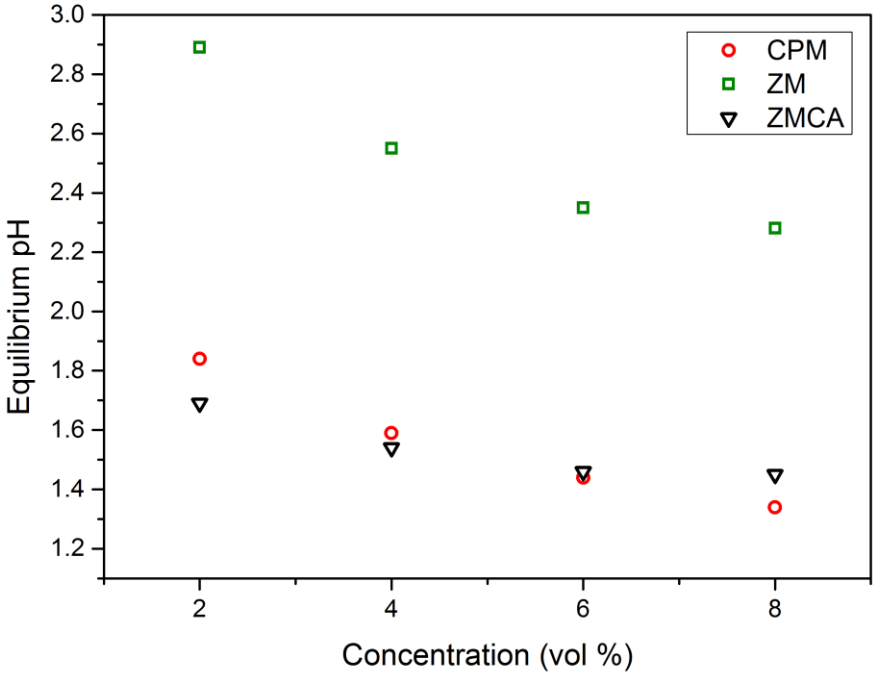

Figure 5: Equilibrium pH (after 48 hours) for CPM, ZM and ZMCA suspensions at various particle concentrations.

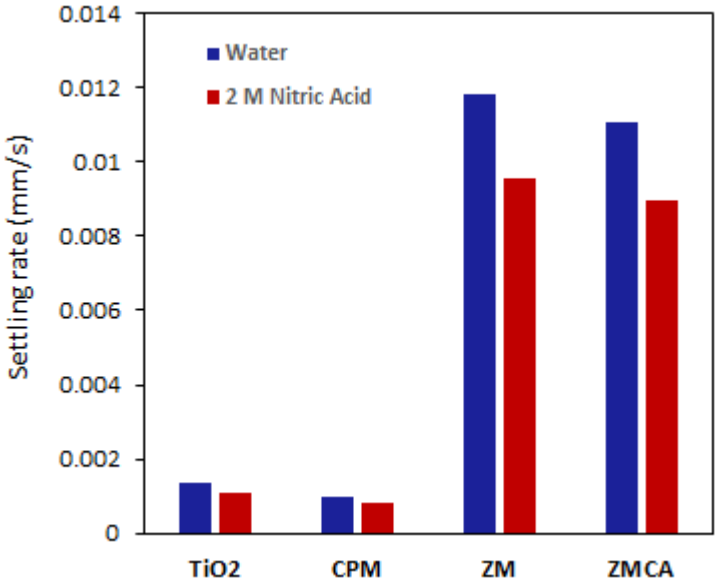

Figure 6: Estimated Stokes settling rates for the studied TiO_2, CPM, ZM and ZMCA particles in water ad 2 M nitric acid.

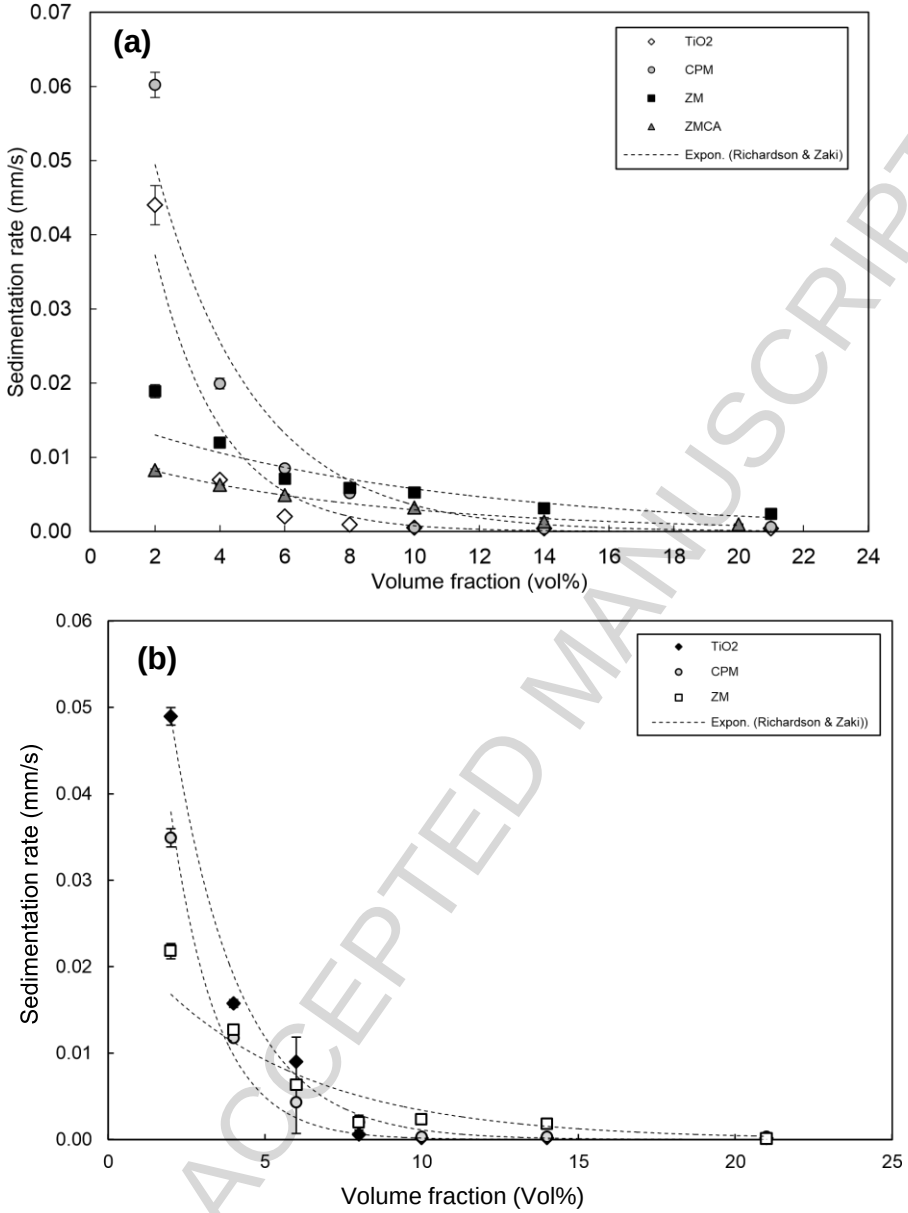

Figure 7: Averaged linear settling rates for TiO_2, CPM, ZM and ZMCA particles versus concentration in (a) water and (b) 2 M nitric acid (no ZMCA in this case). Dotted lines represent Richardson-Zaki power-law fits for each species.

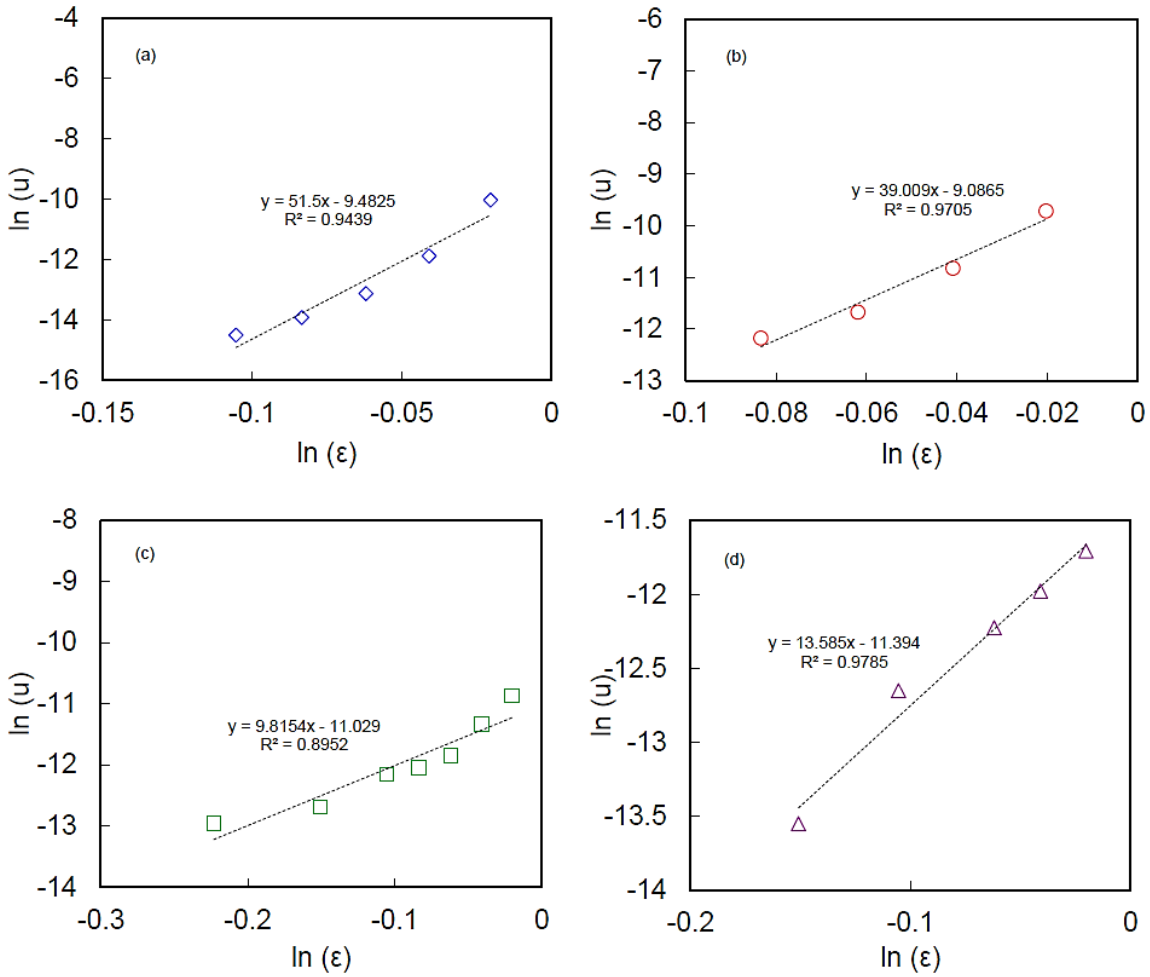

Figure 8: Linearised Richardson-Zaki settling rate fits versus porosity (ε) for (a) TiO_2, (b) CPM, (c) ZM and (d) ZMCA in water.

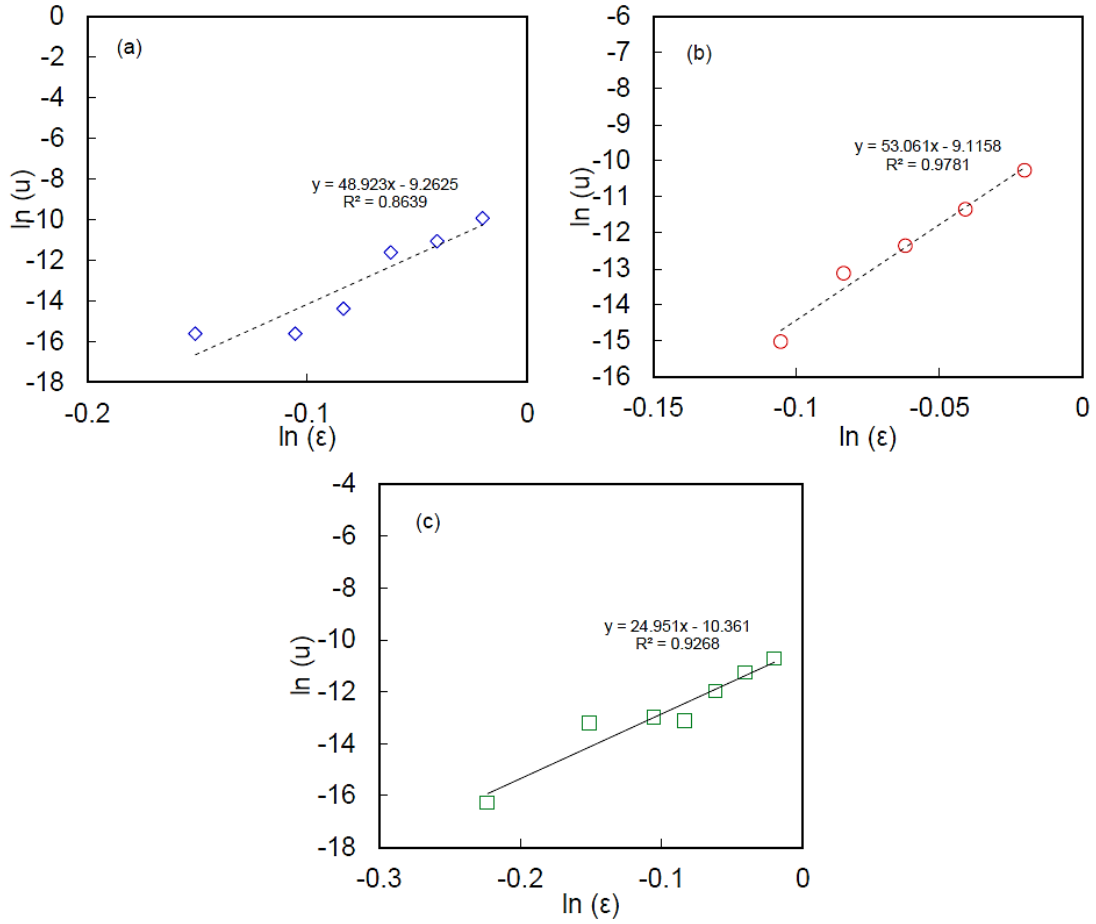

Figure 9: Linearised Richardson-Zaki settling rate fits versus porosity (ε) for (a) TiO_2, (b) CPM and (c) ZM in 2 M nitric acid.

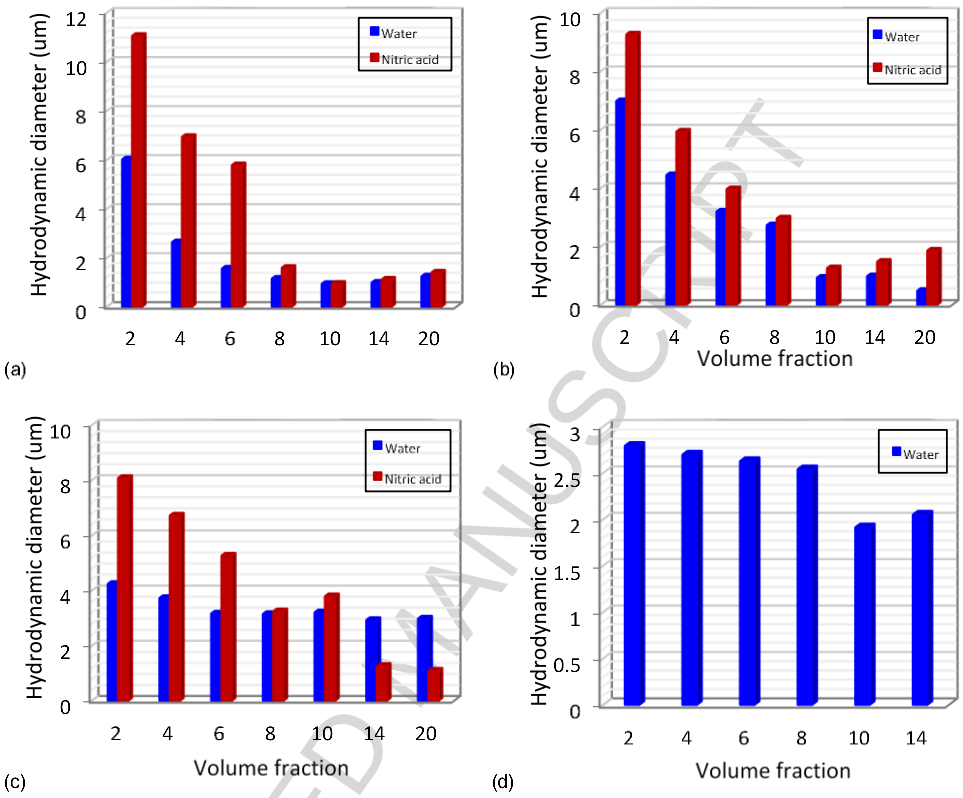

Figure 10: Calculated hydrodynamic diameter (using the modified Stokes equation presented in Eq. 1) at various particle volume fractions in water and 2 M nitric acid, for (a) TiO_2, (b) CPM, (c) ZM and (d) ZMCA (water only).

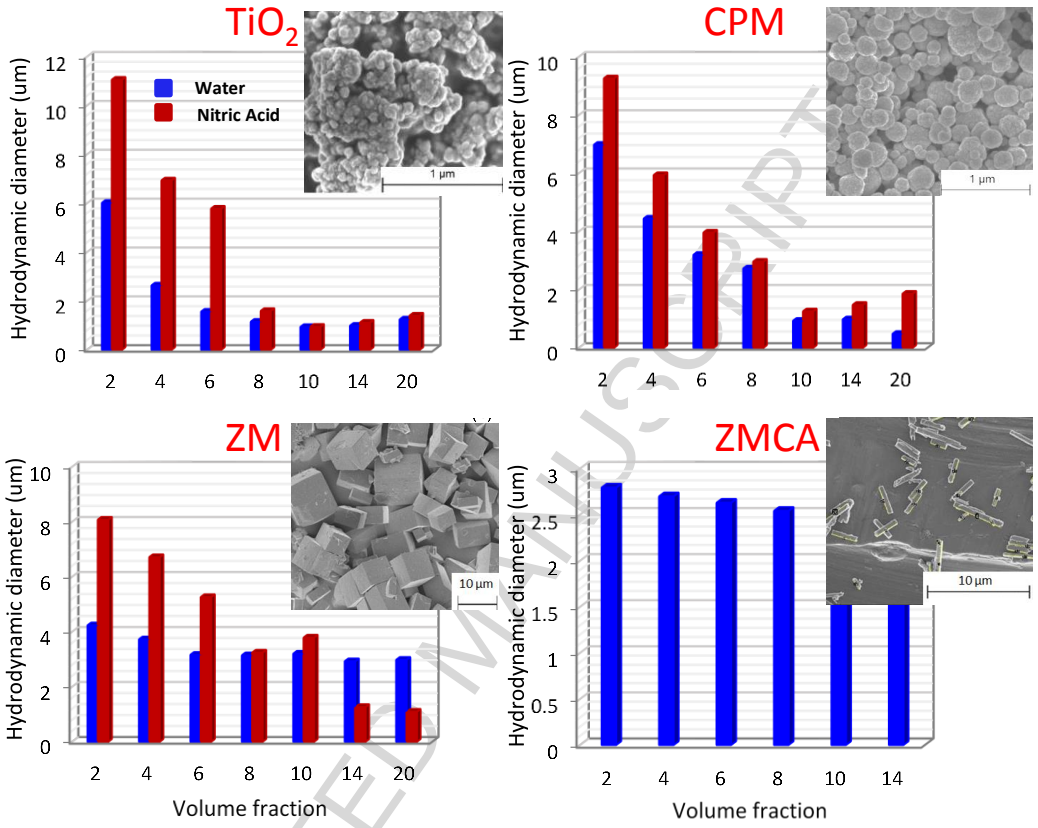

Graphical Abstract

Pow. Tech. – Paper Highlights

- Sedimentation of Spheroidal, cubic and elongated cuboidal particle studied.
- Stable cubic and cuboidal suspensions heightened hindered settling due to shape drag.
- Aggregation of cubic particles evidenced in 2 M acid, enhancing hindered settling.
- Extended Stokes model successful at estimating particle size in stable suspensions.
- Extended Stokes model also a key method for determination of aggregation state.